


ORIGINAL ARTICLE

Evaluation of facial tissue stresses under medical devices post application of a cyanoacrylate liquid skin protectant: An integrated experimental-computational study

Raz Margi | Amit Gefen 

Department of Biomedical Engineering,
Faculty of Engineering, Tel Aviv
University, Tel Aviv, Israel

Correspondence

Amit Gefen, The Herbert J. Berman Chair
in Vascular Bioengineering, Department
of Biomedical Engineering, Faculty of
Engineering, Tel Aviv University, Tel Aviv
6997801, Israel.
Email: gefen@tauex.tau.ac.il

Funding information

Israeli Ministry of Science & Technology,
Grant/Award Number: 3-17421; Medline
Industries, Inc. (Northfield IL, USA)

Abstract

Medical device-related pressure ulcers (PUs) (injuries) are a subclass of PUs, associated with pressure and/or shear applied by a medical device onto the skin. Clinical application of a cyanoacrylate liquid skin protectant (CLSP) under the contours of skin-contacting medical devices to shield an intact skin from the sustained mechanical loads that are applied by medical devices is a preventative option, but no computer modelling work has been reported to assess the biomechanical efficacy of such interventions. Here, we investigated the biomechanical protective effect of a polymerised cyanoacrylate coating using three-dimensional, anatomically realistic finite element models of the ear with oxygen cannula and the mouth with endotracheal attachment device, informed by experimental studies. We have compared tissue stress exposures under the devices at these facial sites between conditions where the cyanoacrylate skin protectant has been applied or where the device was contacting the skin directly, without the shielding of the cyanoacrylate coating. The CLSP considerably reduced the skin stress concentration levels and overall tissue stress exposures under the aforementioned medical devices. This demonstrates strong biomechanical effectiveness of the studied cyanoacrylate-based skin protectant in prevention of facial medical device-related injuries at small, curved and thereby difficult to protect facial sites.

KEYWORDS

coefficient of friction, endotracheal tube attachment device, finite element modelling, medical device-related pressure ulcer/injury, oxygen cannula

Key Messages

- Medical device-related pressure ulcers (injuries) are a growing concern
- A cyanoacrylate skin protectant can be applied at skin-device contact regions

This is an open access article under the terms of the Creative Commons Attribution-NonCommercial-NoDerivs License, which permits use and distribution in any medium, provided the original work is properly cited, the use is non-commercial and no modifications or adaptations are made.

© 2021 The Authors. *International Wound Journal* published by Medicalhelplines.com Inc (3M) and John Wiley & Sons Ltd.

- We investigated the biomechanical protective effects of cyanoacrylate coating
- Facial tissue interactions with oxygen delivery devices were modelled
- The studied cyanoacrylate product effectively protects skin and subdermally

1 | INTRODUCTION

Pressure ulcers (PUs) are defined as localised damage to skin and/or underlying tissues as a result of prolonged pressure or pressure in combination with shear.¹ Medical device-related pressure ulcers (MDRPU) are a sub-class of PUs, associated with such pressure and/or shear applied by a medical device onto the skin.² The differential diagnosis is that MDRPUs usually conform to the contours of the specific skin-contacting device that was applied. The incidence and prevalence of MDRPU cases in intensive care units (ICUs) range between 0.9–41.2% and 1.4–121%, respectively, reflecting heterogeneity in data collection and reporting.³ In non-ICU settings, the pooled incidence and prevalence reported in a recent systematic review and meta-analysis are 12% and 10%, respectively.⁴ Facial tissues are commonly affected by MDRPUs as ventilation, assisted breathing, and enteral feeding all require application and attachment of devices and tubing to the head.^{5,6} Accordingly, facial MDRPUs are often reported to be caused by an oxygen cannula above the ear or on the upper lip where an endotracheal tube attachment device (ETAD) has been applied.^{6–11} It is noteworthy that MDRPUs can be easily infected and deteriorate to sepsis and osteomyelitis, which lengthens the hospital stay and increases the healthcare costs and would typically leave severe facial scars with high psychological impact.^{12,13} In addition, being a hospital-acquired injury by definition, MDRPUs are considered a matter of patient safety and healthcare quality and may, therefore, lead to malpractice lawsuits against the facility and healthcare workers involved in the case, also resulting in legal and insurance expenses.^{14–17}

Although nursing staff are often using dressing cuts prophylactically to cushion facial sites at-risk of MDRPUs,¹⁸ this is not always possible or appropriate, particularly at anatomical regions that are small and/or highly curved, with facial sites often presenting the most challenging scenarios. The Marathon cyanoacrylate liquid skin protectant (CLSP) manufactured by Medline Industries Inc. (Northfield, Illinois) consists of cyanoacrylate-based monomers that polymerise when they make contact with moisture on the skin surface. This CLSP chemically bonds to the epidermis, creating a strong, continuous shield to the skin, irrespective of the size or curvature of the region of application.¹⁹ The clinical

literature demonstrates that CLSP is effective in treating fissures and protecting peristomal skin,^{19,20} which confirms recently published theoretical²¹ and laboratory²² results, both demonstrating that CLSP considerably increases the mechanical durability of skin at the sites of application. The mechanisms of action of the CLSP in increasing the durability of skin have been identified in the aforementioned bioengineering work as there is an increase of the flexural stiffness of treated skin and concurrently a decrease of the coefficient of friction (COF) of treated skin with contacting materials.^{21,22} Nevertheless, computer modelling work to test the biomechanical efficacy of CLSP in the specific context of preventing MDRPUs has not been reported thus far.

Here, we present state-of-the-art, anatomically realistic computer models of common facial MDRPUs, specifically associated with use of an oxygen cannula and ETAD, which facilitated detailed and rigorous testing of the protective biomechanical efficacy of the above CLSP in prevention of MDRPUs linked with these devices. Relevant experimental work has been conducted and is reported here, in particular with regard to the COF of treated skin with medical device materials, as this information was unavailable in the literature and was required for the present research to accurately determine the performances of the studied CLSP. The present work provides comprehensive and clinically relevant evidence demonstrating the strong biomechanical efficacy of CLSP in prevention of facial MDRPUs in patients who are in need of breathing support.

2 | METHODS

2.1 | Measurements of the elastic modulus of the polymerised CLSP

To measure the elastic modulus of the polymerised CLSP, uniaxial tensile tests were conducted using an electromechanical testing machine (model 5944, Instron Co., Norwood, Massachusetts). We followed a modified protocol based on the ASTM D882-02 standard test method for determining the tensile properties of thin plastic sheets. A load cell with a measurement range of 0.04 to 10 N and accuracy of $\pm 0.5\%$ has been used. The grip separation speed has been set as 5 mm/min. Given that the CLSP

applicator produces a thin CLSP layer (in the order of a few tens of micrometres),²³ which strongly adheres to substrata onto which it is applied, it was not feasible to test the polymerised CLSP material in isolation. Composite test specimens were therefore produced, by applying the CLSP to rectangular plastic carriers with thickness of 30 μm , grip length of 50 mm, and width of 15 mm. We first tested the above plastic carriers separately (five specimens), and these tests indicated that the elastic modulus of the plastic carriers themselves (E_{pc}) was 103.7 ± 7.2 MPa. The composite test specimen thicknesses ($t_{\text{composite}}$) were in the range of 63 to 86 μm , that is, the thickness of the polymerised CLSP applied above the plastic substrata (t_{CLSP}) was 33 to 56 μm ($N = 5$ specimens), which resembles the thickness of application of this CLSP in real-world conditions.²¹ All the thickness measurements were performed using a micrometre (Holex-421 505, Hoffmann Group Co., Munich, Germany) with resolution of 1 μm , and 18 measurement points were taken per each specimen to account for any potential surface roughness or waviness. We then tested the plastic-CLSP composite specimens under tensile loading using the aforementioned grip separation speed to extract the elastic modulus of the polymerised CLSP (E_{CLSP}), in isolation from that of the plastic carrier, as follows:

$$E_{\text{CLSP}} = \frac{E_{\text{composite}} \cdot t_{\text{composite}} - E_{pc} \cdot t_{pc}}{t_{\text{CLSP}}}, \quad (1)$$

where $E_{\text{composite}}$ is the measured elastic modulus of the plastic-CLSP composite (146 ± 24 MPa). Substituting the abovementioned dimensions and the E_{pc} data in Equation 1 resulted in that the E_{CLSP} is 173 ± 38 MPa.

2.2 | Coefficient of friction studies

We have measured the coefficient of friction (COF) properties of epoxy and native skin tissues, before and after treating these substrata with the present CLSP, against common skin-contacting materials used in medical devices associated with MDRPUs. The protocol of Schwartz et al²⁴ has been followed for the COF measurements described later.

2.2.1 | The substrata for the COF measurements

Three types of COF measurement tests have been performed, differing by the substrate on which the CLSP was applied. The first test type was performed on epoxy sheets, on which the CLSP was uniformly applied. The second test type was performed on avian (femoral) skin that has been thoroughly cleaned from feathers. These

specimens were obtained from animals bred for food and slaughtered 1 day prior to the testing. The aforementioned avian skin samples were kept refrigerated from the time of slaughtering to the time of testing. Of note is that the interfollicular skin of birds consists of the same basic layers as that of mammals, that is, epidermis, dermis, and hypodermis; however, birds have a thin and delicate epidermis compared to other vertebrates, which in the context of the present work can be considered to represent a fragile human skin.²⁵ The avian test specimens were at approximate sizes of 70 \times 70 mm. The CLSP adhered well to all the avian skin specimens and has created a uniform coating layer on each. The third type of COF measurements was performed on fresh porcine skin samples with sizes of 90 \times 180 mm, harvested from the ventral area of a 3-month-old female, local domestic commercial pig, which was used for a different, unrelated acute study. The skin samples were excised from the corpse by an expert surgical veterinarian at the Sheba Medical Center (Ramat-Gan, Israel), under permission (covered in the original study approvals) to excise tissue specimens for further laboratory testing. The samples were extracted immediately after euthanasia and testing commenced within approximately 30 minutes thereafter, thereby avoiding freezing or other potentially destructive methods of tissue preservation. The samples were carefully shaved before the testing. Similarly to its interaction with avian skin, the CLSP adhered well to the porcine skin and was evenly distributed.

2.2.2 | The medical device materials used for the COF measurements

The present COF measurements were performed by allowing the above synthetic and skin tissue materials to frictionally slide against common skin-contacting materials used in medical devices associated with MDRPUs. We specifically tested medical grade polyhexahydrotriazine (PHT), which is used for manufacturing of endotracheal tube (ETT) products; polyvinylchloride (PVC), which is used for production of oxygen cannula products; and low-density polyurethane (PUR) foam, which is commonly used for padding skin-contacting medical devices. All these materials were cut and glued to a flat metallic surface, onto which a circular steel weight (170 g) was applied to ensure tight contact conditions with the aforementioned interfacing substrata.

2.2.3 | The measurements of the coefficients of friction for the medical device materials

All the present COF measurements were conducted using an electronically controlled tilting table tribometre

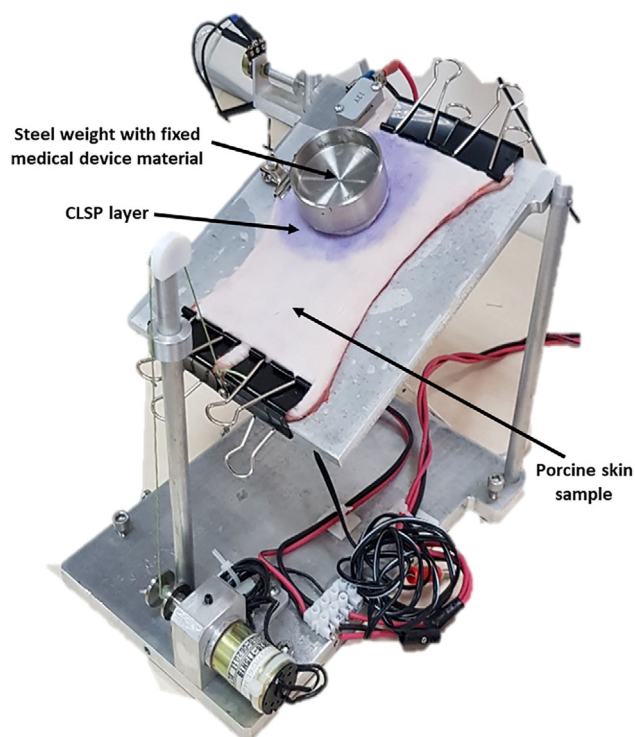


FIGURE 1 Measurements of the coefficient of friction of porcine skin treated with a cyanoacrylate liquid skin protectant in interaction with medical device materials: the tilting table tribometre system

(Figure 1), which has been developed in-house and was used in our previously published work.²⁴ A test specimen with substrate of either epoxy or (avian/porcine) skin tissue was mounted on the plate of the tilting table and a medical device material fixed to the inferior surface of the circular steel weight was applied on top of the said specimen (Figure 1). The angle of the plate of the tilting table was then gradually and slowly increased, by means of a computer-controlled electrical motor. When sliding of the weight initiated, an electrical switch opened instantaneously, causing the motor to immediately stop. The friction angle (θ), which is the angle of the plate at which frictional sliding had started, was then measured using an inclinometer (smartphone application) software; this inclinometer was carefully calibrated at the start of each set of experiments. For each set of reported COF properties, at least five measurements were performed, and the static COF was calculated as $\tan(\theta)$.

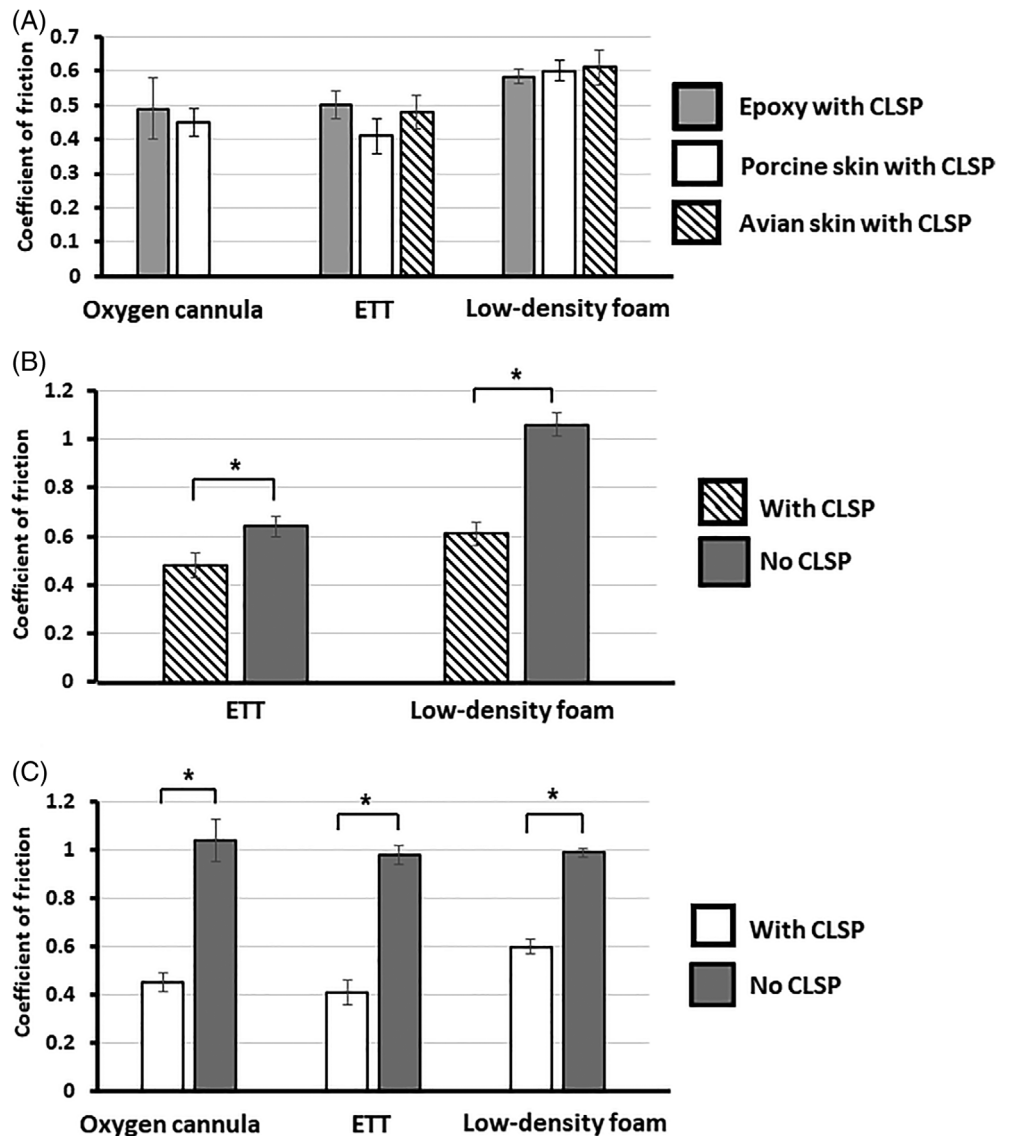
The first test type was performed on the CLSP-treated epoxy sheets to identify any potential dependencies of the measured COF on the type of the substrate onto which the CLSP has been applied. In other words, we sought to compare the COF of the CLSP applied on epoxy with that of CLSP applied to skin (in interaction with the different medical device materials) to determine if the CLSP forms

a sufficiently solid and stiff coating layer so that the frictional interactions occur between the CLSP and medical device materials, regardless of the underlying (tissue) materials.

The second and third types of friction tests were performed using avian and porcine skin, respectively, to test the potential reduction in the static COF due to application of the CLSP on these skin specimens. Although we have tested avian skin here, due to its thin epidermis (which is relevant to fragile human skin as mentioned earlier), we considered the porcine tests as the ones that are most representative of common patient conditions, for two main reasons: (a) porcine tissues are mammalian, and (b) fresh porcine skin is a well-established model for human skin in the wound care literature. Accordingly, for the porcine skin tests, we controlled the ambient conditions as well: the temperature and relative humidity were carefully maintained at 25°C and 70%, respectively. At least five repetitions were conducted for each COF test of a certain medical device material in contact with skin (avian or porcine) and each such set was conducted with the CLSP applied as a barrier between the device material and skin, and also when no CLSP was present, for the purpose of statistical comparisons. For the latter statistical comparisons, we ran unpaired, two-tailed *t*-tests, separately per each skin type and for all kinds of the studied medical device materials, to determine whether the effect of the CLSP treatment on skin (avian or porcine) had significantly reduced the static COF. A *P* value lower than 0.05 was considered statistically significant.

The results of all the above-mentioned COF studies, used as input data for the computational modelling work as described further later, are plotted in Figure 2. The effects of the substrate type on the static COF of the CLSP were statistically indistinguishable, as epoxy and skin substrata treated with the present CLSP yielded similar COF values in interaction with each specific device material (Figure 2A), indicating that the frictional sliding interaction had always occurred between the CLSP coating and the device material. Treating the skin specimens with the CLSP significantly reduced the static COF for both the avian (Figure 2B) and porcine (Figure 2c) skin ($P < 0.01$). For the porcine skin studies, which we consider here as the most representative ones in the context of human PU research given the structural and physiological similarities of pig skin to human skin, we found that application of the CLSP reduced the static COF by 57%, 58%, and 39% for the PVC, PHT, and PUR device material types, respectively ($P < 0.01$). These percentage reductions (Figure 2B) have been used in our further modelling work reported later.

FIGURE 2 The coefficient of friction (COF) experimental data: A, comparison between the COF of medical device materials in contact with synthetic epoxy substrate, avian skin, and porcine skin coated with a cyanoacrylate liquid skin protectant (CLSP). B, The COF of avian skin with/without application of CLSP. C, The COF of porcine skin with/without CLSP. Error bars are the SDs from the mean; * $p < 0.05$ in unpaired, two-tailed *t*-tests. ETT, endotracheal tube



2.3 | Computational modelling of application of medical devices on facial sites

2.3.1 | The modelled facial anatomical areas and their geometry reconstructions

Two different finite element (FE) models were developed in this work to study common facial MDRPUs in patients: (a) an ear model in interaction with an oxygen cannula; (b) a mouth region model in interaction with an ETAD. Application of CLSP has been simulated in both model types, which facilitated standardised comparisons of the facial tissue loading states at each facial site post application of the CLSP versus the (reference) no-CLSP condition.

Both the ear and the mouth region models were created using the Scan-IP module of the Simpleware

segmentation software package²⁶ (Synopsys, Mountain View, California) based on the Visible Human (male) Project image database.²⁷ The ear model (Figure 3) incorporated the relevant detailed three-dimensional anatomy of the left ear with segmented skin and cartilage structures, along with subdermal fat and skull bone of that region. The total volume of the ear model was $40 \times 75 \times 88$ mm. An oxygen cannula with its support tube has been added above the (left) ear at its clinically relevant position, which is where MDRPUs associated with this particular device are frequently reported (Figure 3A). The inner and outer diameters of the support tube of the aforementioned oxygen cannula were 2 mm and 3 mm, respectively²⁹ (Figure 3B). The length of the modelled segment of this support tube was 20 mm (Figure 3B), which allowed the mechanical boundary conditions to apply far enough from the tube-skin contact area.

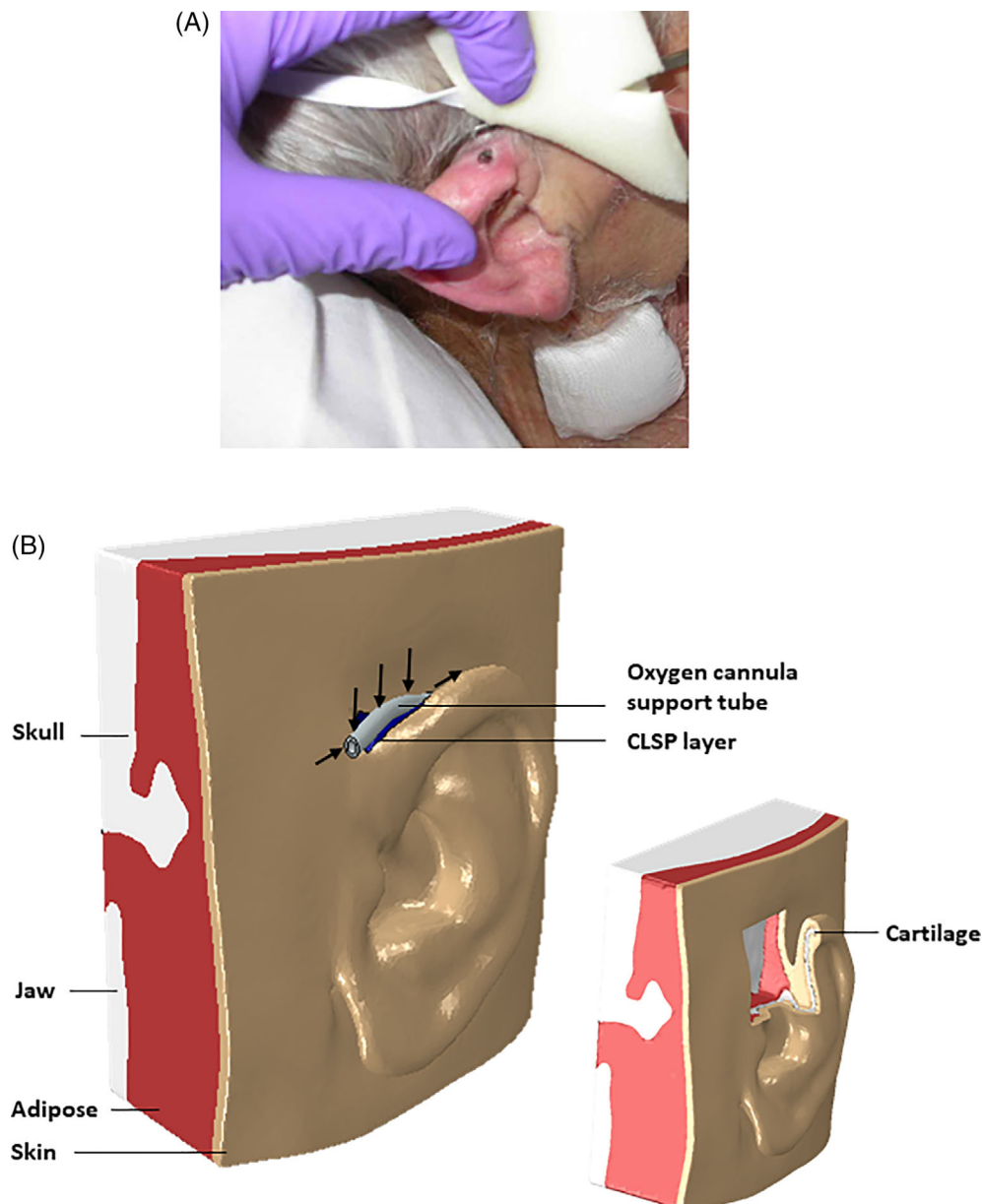


FIGURE 3 The ear injury model: A, clinical presentation of a device-related pressure ulcer caused by an over-the-ear oxygen nasal cannula.²⁸ B, Computational (finite element) modelling of the interaction between the left ear and an oxygen cannula support tube. The geometrical configuration and the pressure and shear loading conditions that are forming between the tubing and skin are shown. CLSP, cyanoacrylate liquid skin protectant

The second model type, of the mouth region (Figure 4), was based on previously published facial modelling work of our group,³⁰⁻³² which has been adapted for the purposes of the current study. Similarly, we chose to model a common MDRPU scenario caused by interaction of the skin above the upper lip with an ETAD (Figure 4A). The volume of the mouth region model was $77 \times 82 \times 89$ mm. An anchoring support foam, which is part of the ETAD kit, has been added on the facial skin in this model type, again at its clinically-relevant position, above the upper lip (Figure 4B), with dimensions of $22 \times 10 \times 5$ mm, which represents sizes of commercial ETADs.

Application of a 20- μ m-thick¹⁹ layer of CLSP has been considered in each of the two model types (ear and mouth). However, in order to determine the

potential influence of the thickness of the applied CLSP coating on the tissue loading states and as part of our sensitivity analyses, we have also examined additional ear model variants where the CLSP layers were 40 μ m and 60 μ m thick. In clinical practice terms, these thicker CLSP layers would represent topical re-application of the CLSP, twice or three times, respectively, at layers that are 20 μ m thick at each time of application.

The dimensions of the CLSP region for the ear model were approximately 15×7 mm, representing minimal application of this intervention under the oxygen cannula support tube (Figure 3). Likewise, the CLSP layer on facial skin above the upper lip in the mouth region model represented a minimum application area of 30×12 mm under the anchoring foam of the ETAD.

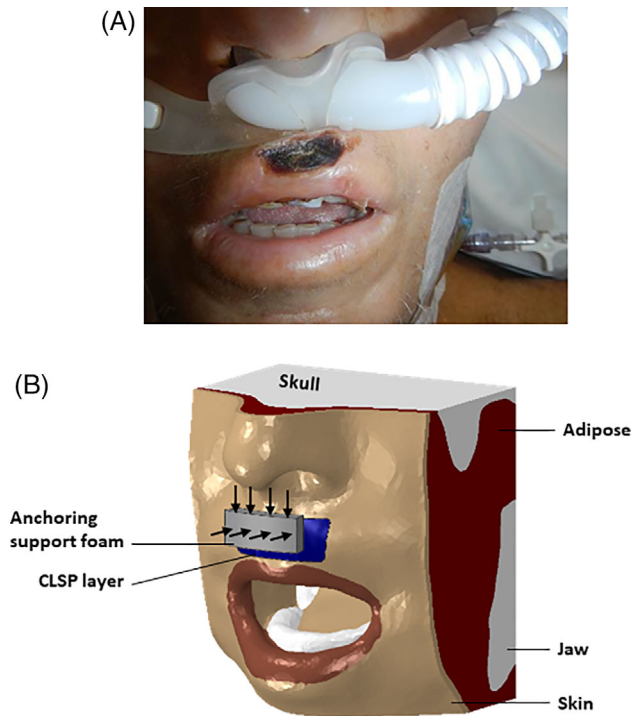


FIGURE 4 The lip injury model: A, clinical presentation of a device-related pressure ulcer caused by an endotracheal tube attachment device (ETAD).

The image is courtesy of Dr Michelle Barakat-Johnson (The University of Sydney) and Thomas Leong (Royal Prince Alfred Hospital) of New South Wales, Australia. B, Computational (finite element) modelling of the interaction between the facial tissues above the upper lip and an ETAD. The geometrical configuration and the pressure and shear loading conditions that are formed between the ETAD and skin are shown. CLSP, cyanoacrylate liquid skin protectant

2.3.2 | Mechanical behaviour and properties of the model components

The material models and properties used in both FE model types are specified in Table 1. The skull and mandible bones were assumed to be isotropic and linearly elastic materials. All the soft tissues of the face excluding skin (ie adipose, ear cartilage, lips, and mucosa tissues) and all the synthetic polymer materials (ie the oxygen cannula support tube, the anchoring support foam, and the CLSP) were assumed to behave as isotropic and hyperelastic neo-Hookean materials with a strain energy density function⁴³ as follows:

$$W = \frac{\mu}{2}(\bar{I}_1 - 3) + \frac{1}{D_1}(J - 1)^2, \quad (2)$$

where μ and D_1 are material-specific properties (Table 1), \bar{I}_1 is the first deviatoric strain invariant, and $J = \det(F)$

where F is the deformation gradient tensor. Skin tissues in both model types were assumed to be isotropic and to obey the following hyperelastic, second-order Ogden strain energy density function⁴³:

$$W = \sum_{k=1}^2 \frac{2\mu_k}{\alpha_k^2} (\bar{\lambda}_1^{\alpha_k} + \bar{\lambda}_2^{\alpha_k} + \bar{\lambda}_3^{\alpha_k} - 3) + \frac{1}{D_1}(J - 1)^2, \quad (3)$$

where $\bar{\lambda}_i = J^{-\frac{1}{3}}\lambda_i$ are the deviatoric principal stretches; $J = \det(F)$; and μ_k , α_k , and D_1 are the material-specific properties reported by Flynn and colleagues, based on their in vivo experiments in human facial skin.³³ For sensitivity analyses (conducted for the ear model), we further considered a possible $\pm 30\%$ variation in the value of the aforementioned μ_k parameter to account for the well-documented biological variability and age-related changes in skin stiffness.⁴⁴

The elastic modulus of the CLSP has been determined as the mean empirical E_{CLSP} value measured in our CLSP mechanical characterisation experiments described above (in Section 2.1). However, for the ear model and as part of our present sensitivity analyses, we have also considered variations of ± 2 SDs around the mean measured E_{CLSP} value, to account for nearly the entire range of possible stiffness outcomes of the polymerisation of the CLSP on skin (again reflecting the potential impact of biological variability in skin responses). In both model types, all the soft tissues were assumed to be nearly incompressible, with a Poisson's ratio of 0.495.

2.3.3 | Boundary conditions and interfaces

Displacement boundary conditions for the ear model included 3.5 mm-downward and 2 mm-horizontal displacements that were applied on the support tube against the superior surface of the ear. An upward reaction force of 0.55 N (~ 56 g), which formed between the support tube and the ear, was considered for the comparison of the tissue-loading states between the simulation with the applied CLSP and the one with no CLSP. Boundary conditions for the mouth region model included displacements of the anchoring support foam by 4 mm and 3 mm perpendicularly and in parallel to the skin surface, respectively. For the mouth region model, the (upward) reaction force level for comparison of the tissue loading states in the model variants with versus without the CLSP was chosen to be 0.6 N (~ 61 g). The back surfaces of both the ear model (Figure 3) and the mouth region model (Figure 4) were fixed for all translations and rotations. The other cross-sectional surfaces in both model

TABLE 1 Mechanical properties and elemental data for all the finite element model components

Model component	Material model	Material properties	Number of mesh elements		
			Ear model	Upper lip model	
Skin ^a	Second-order Ogden	$\alpha_1 = 2.1, \alpha_2 = 35.24$ $\mu_1 = 50.4$ (kPa), $\mu_2 = 0.0003$ (kPa), $D_1 = 0.0004 \left[\frac{1}{\text{kPa}} \right]$	171 064	139 967	
		Instantaneous shear modulus, μ (kPa)			
		Poisson's ratio, ν			
Adipose ^b	Neo-Hookean	0.286	0.495	187 332	199 834
Ear cartilage ^c	Neo-Hookean	381	0.495	47 432	—
Lips and mucosa ^{d,e}	Neo-Hookean	11.2	0.495	—	81 856
CLSP layer	Neo-Hookean	59.1×10^3	0.46^f	4458	7635
Skull ^g	Elastic	2.701×10^6	0.2	54 480	65 084
Mandible ^h	Elastic	2.03×10^6	0.23	10 158	15 498
Oxygen cannula support tube	Neo-Hookean	1.1×10^{31}	0.364^i	43 890	—
Anchoring support foam ^k	Neo-Hookean	5.9	0.3	—	7372

Abbreviation: CLSP, cyanoacrylate liquid skin protectant.

^aFlynn et al.³³

^bSopher et al.³⁴

^cBos et al.³⁵

^dLuboz et al.³⁶

^eGefen and Haberman et al.³⁷

^fFerreira et al.³⁸

^gMoore et al.³⁹

^hHorgan et al.⁴⁰

ⁱThompson US patent 7614401.²⁹

^jKoda et al.⁴¹

^kPeko et al.⁴²

types were constrained for any normal movements, for achieving numerical stability.

Frictional sliding was defined in the ear model at the contact site between the support tube of the oxygen cannula and the skin of the superior ear. Likewise, frictional sliding was also defined at the contact region between the anchoring support foam and the skin above the upper lip. The literature specifies that the COF of the support tube material with dry skin is 0.55,⁴⁵ and that of the anchoring foam material with dry skin is 0.7.⁴⁶ The percentage reductions of COF values due to application of the CLSP, as reported in this work for fresh porcine skin, have therefore been applied to extrapolate the reductions of the COF of the above synthetic materials with human skin once the CLSP is present on human skin. The empirical data reported in Figure 2 indicate that the reduced COF values post application of the CLSP are 0.24 (with respect to the 0.55 value for no-CLSP) and 0.43 (with respect to the 0.7 value for no-CLSP), for the support tube of the oxygen cannula on ear skin and for the anchoring foam on facial skin above the upper lip, respectively.

2.3.4 | Numerical methods

Four-node linear tetrahedral elements were used to mesh the volumes of all the hard and soft tissues in both model types. Both models were meshed using the Scan-IP module of Simpleware²⁶ and finer meshes were produced locally where needed, particularly in and around areas of device-skin contacts and within each volume of interest (VOI) that was defined for calculation of stress outcome measures (as reported further below). For meshing the CLSP, 3-node triangular shell elements were used in both model types; the CLSP elements were tied to the skin mesh beneath it. The support tube for the oxygen cannula and the anchoring foam for the ETAD were created and meshed using the ABAQUS CAE 2020 software (Dassault Systems, Vélizy-Villacoublay, France), using 8-node and 20-node brick elements, respectively. The numbers of elements for each of the model components are specified in Table 1. All the simulation cases described here were solved by means of the ABAQUS CAE 2020 FE solver. The runtimes of the simulations were up to 2 hours, using a 64-bit Windows 10-based

workstation with an Intel core i7-9700CPU 3.00 GHz central processing unit and 32 GB of random access memory.

2.3.5 | Outcome measures

Volumetric tissue exposure to effective stresses was selected as the primary outcome measure for evaluating the biomechanical protective effect of the CLSP on skin and subdermal tissues, consistent with our other published work in the field of PU prevention.^{18,31,47-54} For

both model types (ear and mouth), and in each variant (with CLSP versus no CLSP), volumetric soft tissue exposures to effective stresses were calculated and plotted for visual and quantitative comparisons of the tissue loading states post application of the CLSP versus the no-CLSP case. To facilitate such systematic comparisons, VOIs were defined for both the ear and mouth models; the VOI in each model type is the volume of soft tissues under and around the contact region with the relevant medical device (Figures 5-10). For the ear model, we have distinguished the exposure of skin from the exposure of cartilage to stresses and have analysed and reported these

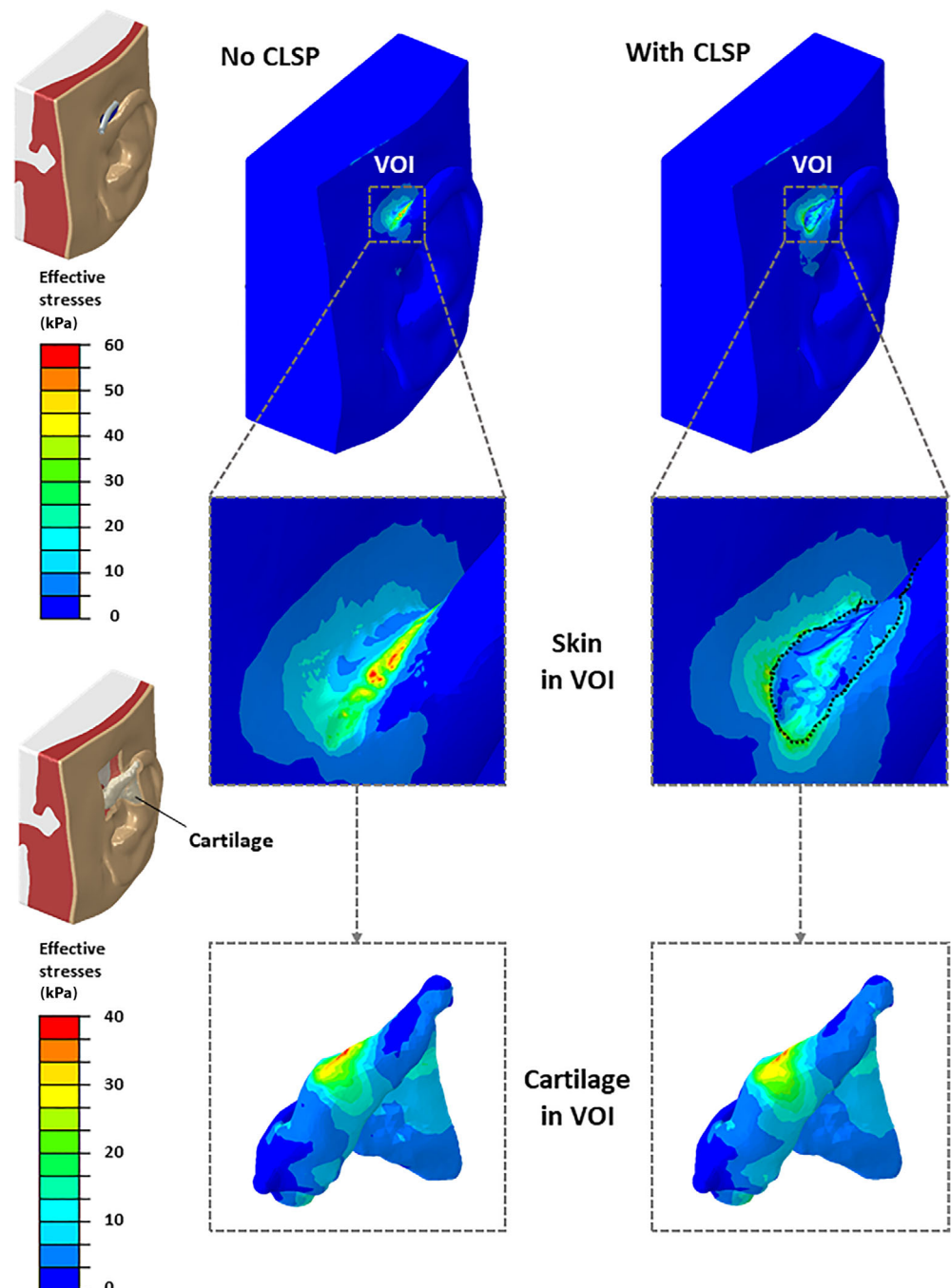


FIGURE 5 Effective soft tissue stress distributions in the ear under the tubing, shown from a superior view (in the top row frames), with (right column) versus without (left column) application of the cyanoacrylate liquid skin protectant (CLSP). Regions where tissue stress concentrations develop are magnified and bounded by dashed frames, which define the volume of interest (VOI) for skin (centre row) and cartilage (bottom row) to facilitate the further analyses. The boundaries of the applied CLSP layer are marked with a dotted line (mid right frame)

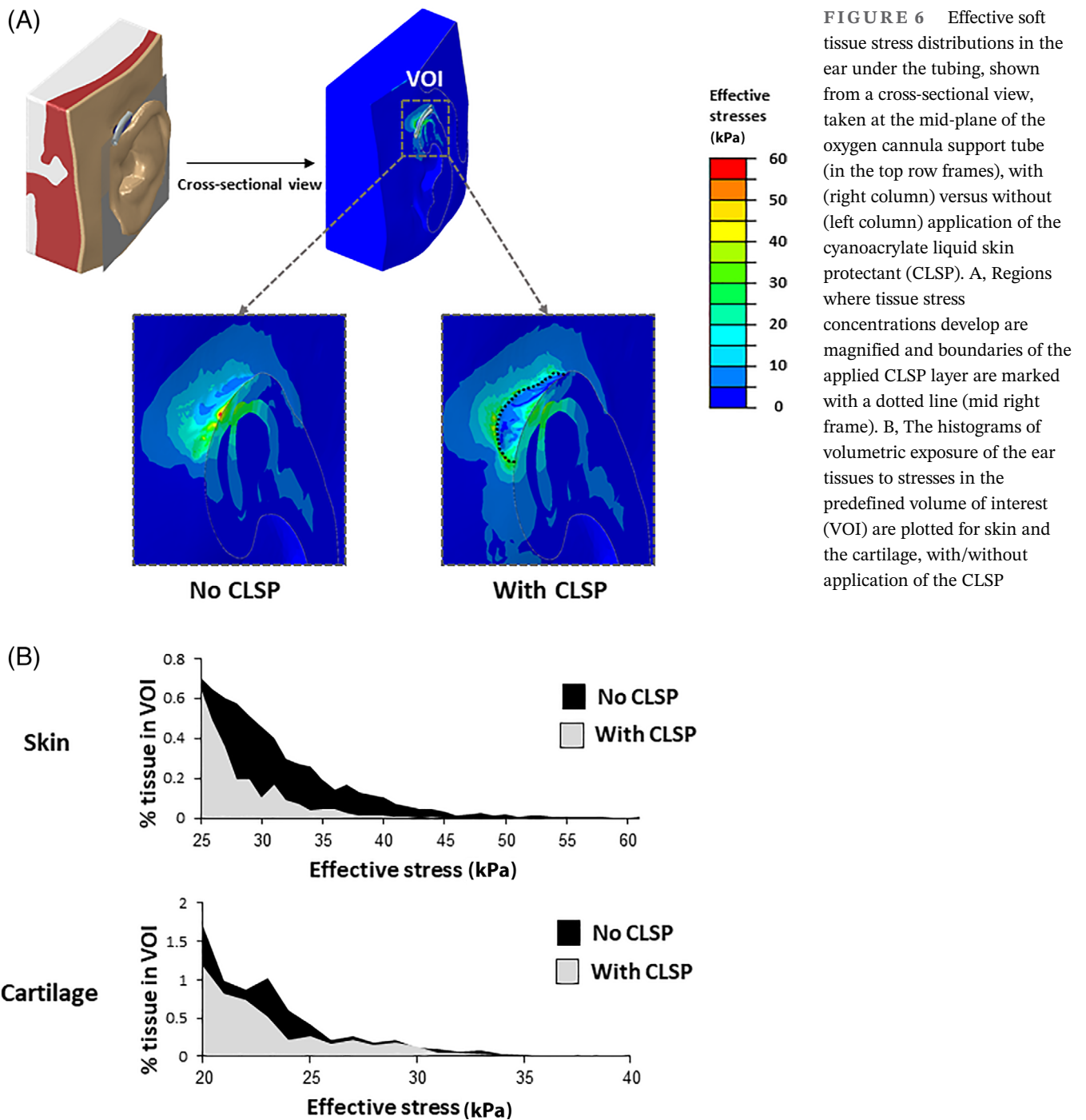


FIGURE 6 Effective soft tissue stress distributions in the ear under the tubing, shown from a cross-sectional view, taken at the mid-plane of the oxygen cannula support tube (in the top row frames), with (right column) versus without (left column) application of the cyanoacrylate liquid skin protectant (CLSP). A, Regions where tissue stress concentrations develop are magnified and boundaries of the applied CLSP layer are marked with a dotted line (mid right frame). B, The histograms of volumetric exposure of the ear tissues to stresses in the predefined volume of interest (VOI) are plotted for skin and the cartilage, with/without application of the CLSP

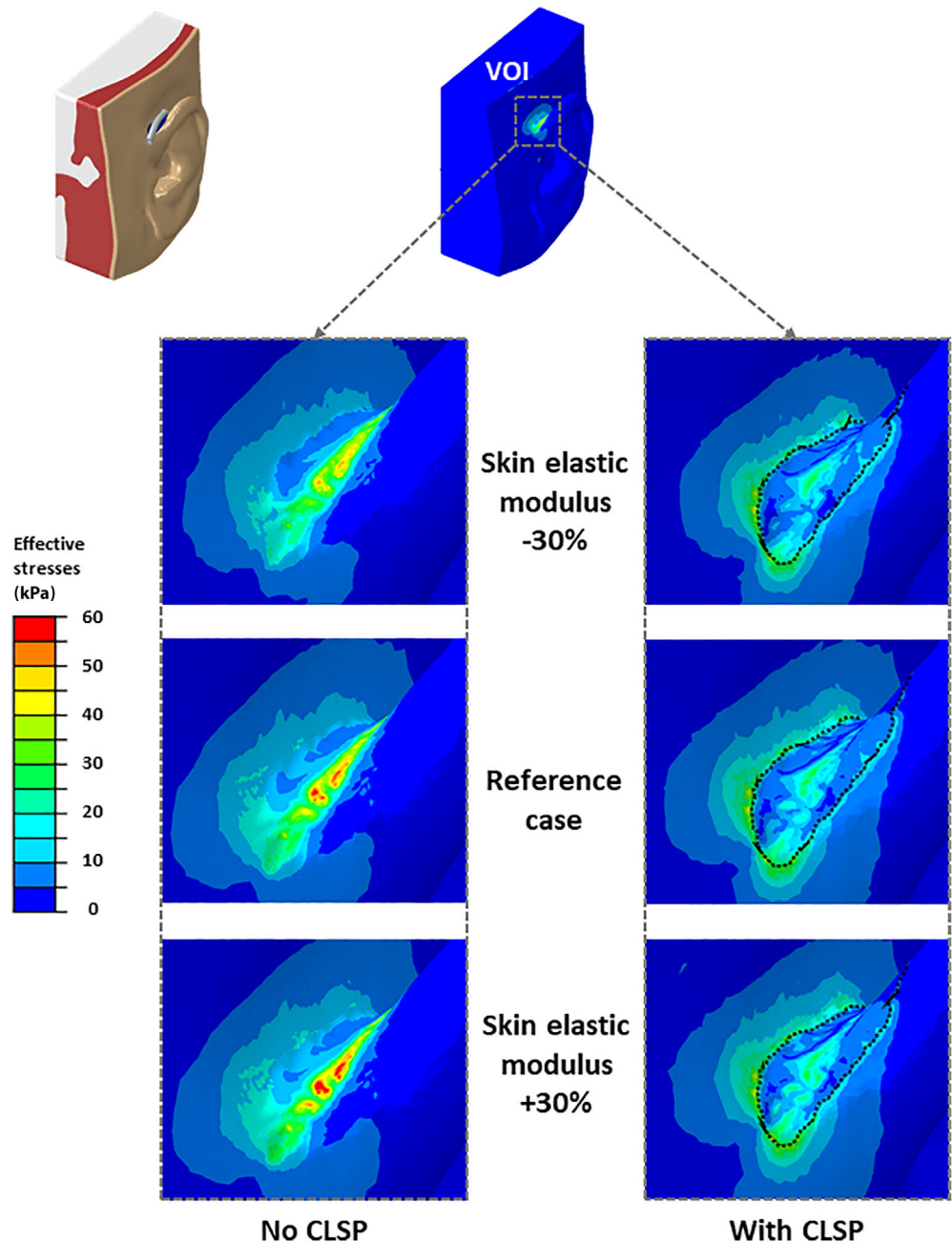
tissue stress exposures separately for the different tissue types. This allowed us to isolate the effect of the CLSP on skin from its potential effects on the loading state of the deep tissue structures of the ear. Given that a MDRPU will most likely form where the stress levels are the highest, we further report the percentage soft tissue volumes (from the VOIs), which are exposed to effective stress values above the median and above the fourth quartile of the stress domain in the respective VOI, per each model type (Tables 2–4).

3 | RESULTS

3.1 | The ear model

The effective stress distributions developed in the tissues of the ear model are shown in Figure 5. The stress concentrations that form under the oxygen cannula support tube are clearly visible; skin (middle frames) and cartilage (bottom frames) in the VOIs have been magnified for detail. The CLSP was able to reduce the skin stresses

FIGURE 7 Sensitivity of the stress levels in skin under the tubing to the skin stiffness value, for a $\pm 30\%$ variation in the elastic modulus of skin (with respect to the reference skin stiffness case), in model variants where the cyanoacrylate liquid skin protectant (CLSP) is applied (right column) versus the corresponding no-CLSP conditions (left column). The boundaries of the applied CLSP layer are marked with a dotted line (on the frames in the right column)



by approximately 40% with respect to the no-CLSP case (middle frames), but the cartilage stresses were slightly affected (bottom frames). Quantitative analyses of the dermal and subdermal volumetric tissue stress exposures in the ear model for the CLSP versus the no-CLSP cases are provided in Figure 6. The CLSP was shown to be effective in reducing the volumetric exposure of ear tissues to stress across the entire stress domain, again with a more profound influence on skin (Figure 6A) than on cartilage (Figure 6B). For skin, in particular, the protective effect of the CLSP increased for stresses above 25 kPa; skin stress peaks above 45 kPa, which existed for the no-CLSP case disappeared following application of the CLSP in the

modelling (Figure 6A). The cumulative volumetric tissue exposures to effective stresses in the VOIs are specified in Table 2. The CLSP has been shown to reduce skin stresses above the median stress value (30 kPa) and above the fourth-quartile stress value (45 kPa) by $\sim 80\%$ and $\sim 97\%$, respectively. Consistent with the visual information in Figures 5 and 6, for cartilage, the decrease in stress values is not so dramatic but is still considerable. Specifically, the CLSP lowered the cartilage stresses above the median stress value (20 kPa) and above the fourth-quartile stress value (30 kPa) by $\sim 31\%$ and $\sim 25\%$, respectively.

The sensitivity analyses of the ear model to variations in the skin stiffness properties are depicted in Figure 7

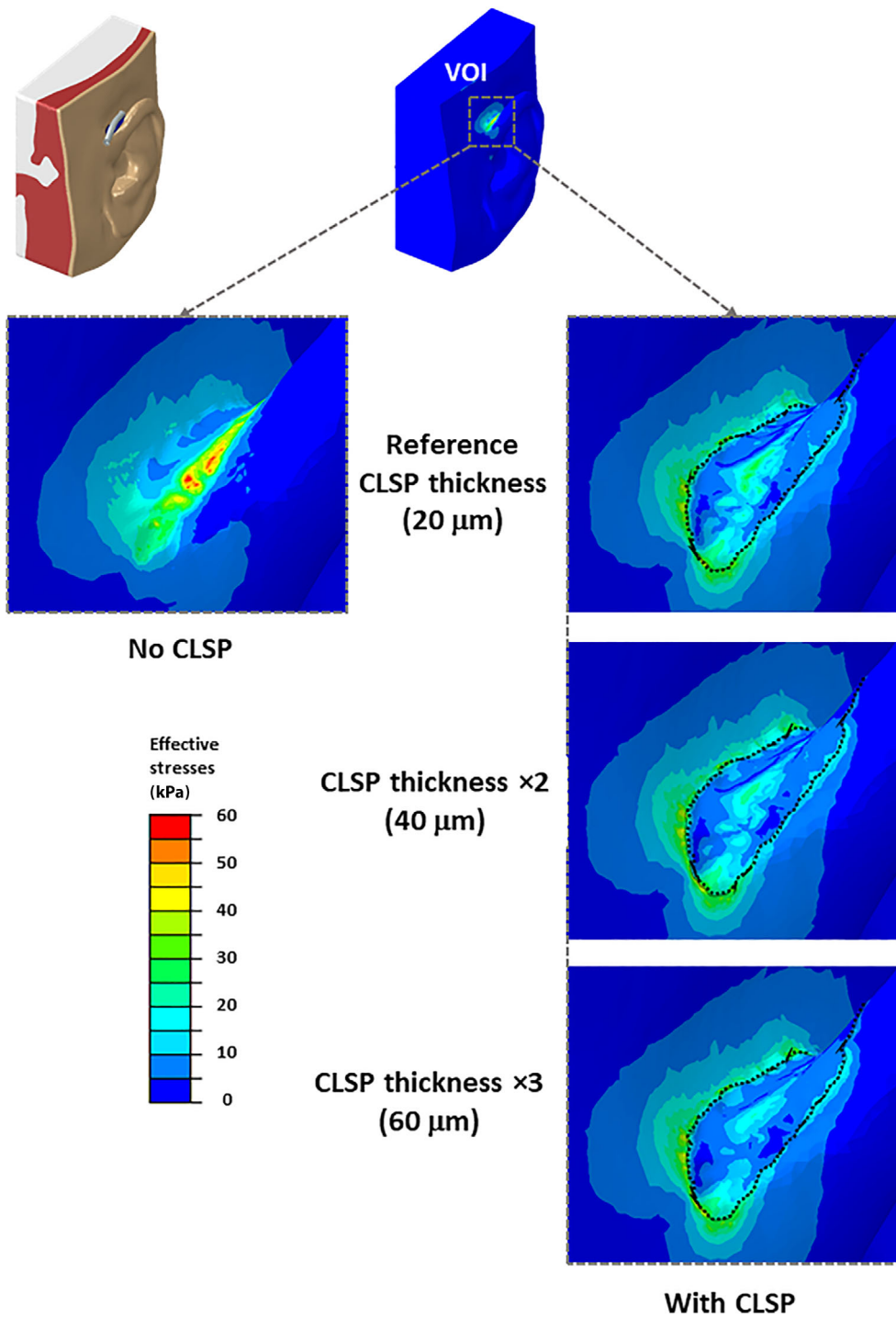


FIGURE 8 Sensitivity of the stress levels in skin under the tubing to the thickness of the cyanoacrylate liquid skin protectant (CLSP) layer, for $\times 1$, $\times 2$, and $\times 3$ thickness variations (with respect to the Reference $20\text{-}\mu\text{m}$ CLSP layer thickness case; top frame in the right column), in model variants where the (CLSP) is applied (right column) versus the no-CLSP condition (left frame). The boundaries of the applied CLSP layer are marked with a dotted line (on the frames in the right column)

and numerically reported in Table 3. These analyses demonstrated that the CLSP is similarly effective in reducing the skin stress levels under the oxygen cannula for the entire tested range of skin stiffnesses, including where the skin stress concentrations were especially elevated, which occurred for the stiffest ($+30\%$) skin condition (bottom frames) (Figure 7). On the contrary, changes in the stiffness of the CLSP itself, representing potential variations in the extent of the polymerisation process associated with the biological variability in individual skin

responses, only had a slight effect on the protective efficacy, that is, within a 3% range for stresses above the median level and unnoticeably for stresses above the fourth-quartile value (Table 3). Testing for the effect of the thickness of the applied CLSP layer (Figure 8) yielded a trend of further moderate reduction in the stress concentration levels where the thickness grew from $20\text{ }\mu\text{m}$ to $60\text{ }\mu\text{m}$: Stresses above the median level reduced by up to additional 10%; stresses above the fourth-quartile value negligibly improved. Since these were

FIGURE 9 Effective soft tissue stress distributions in the upper lip skin under the endotracheal tube attachment device, with (right column) versus without (left column) application of the cyanoacrylate liquid skin protectant (CLSP). Regions where tissue stress concentrations develop are magnified and bounded by dashed frames, which define the volume of interest for skin (bottom row) to facilitate the further analyses. The boundaries of the applied CLSP layer are marked with a dotted line (bottom right frame)

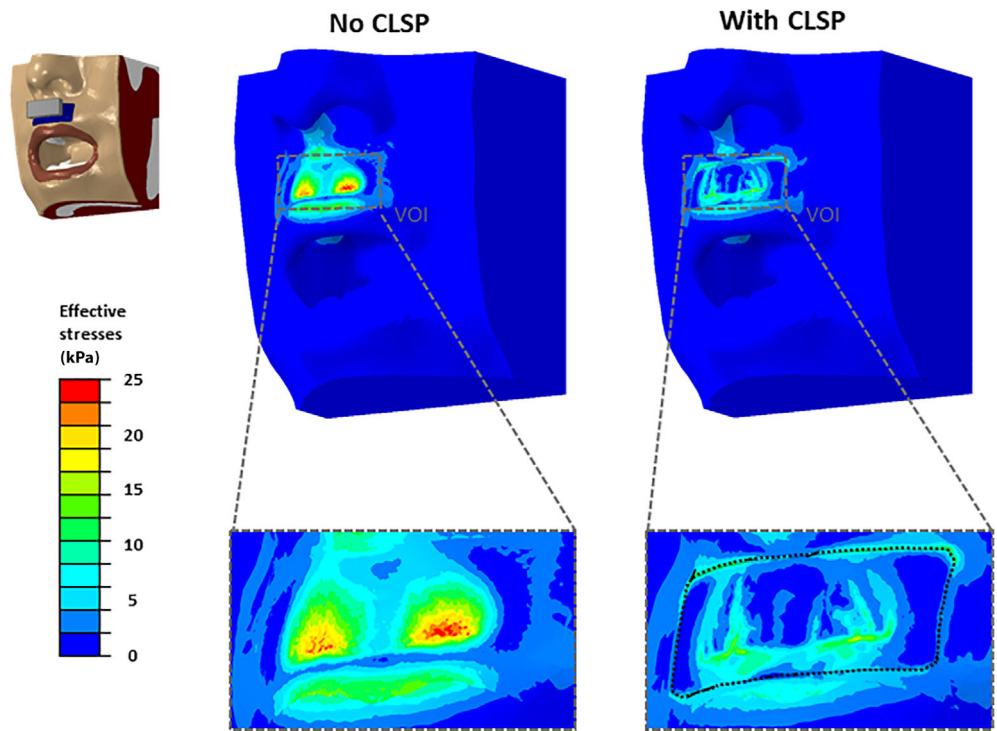


FIGURE 10 Effective soft tissue stress distributions in the upper lip skin under the endotracheal tube attachment device (ETAD), shown from a cross-sectional view, with (right column) versus without (left column) application of the cyanoacrylate liquid skin protectant (CLSP). A, Regions where tissue stress concentrations develop are magnified and boundaries of the applied CLSP layer are marked with a dotted line (bottom right frame). It is shown that the surface stress concentrations spread from the ETAD-skin contact region into the depth of the tissue. B, The histograms of volumetric exposure of skin to stresses in the predefined volume of interest (VOI) are plotted for the case where CLSP has been applied versus the no-CLSP condition

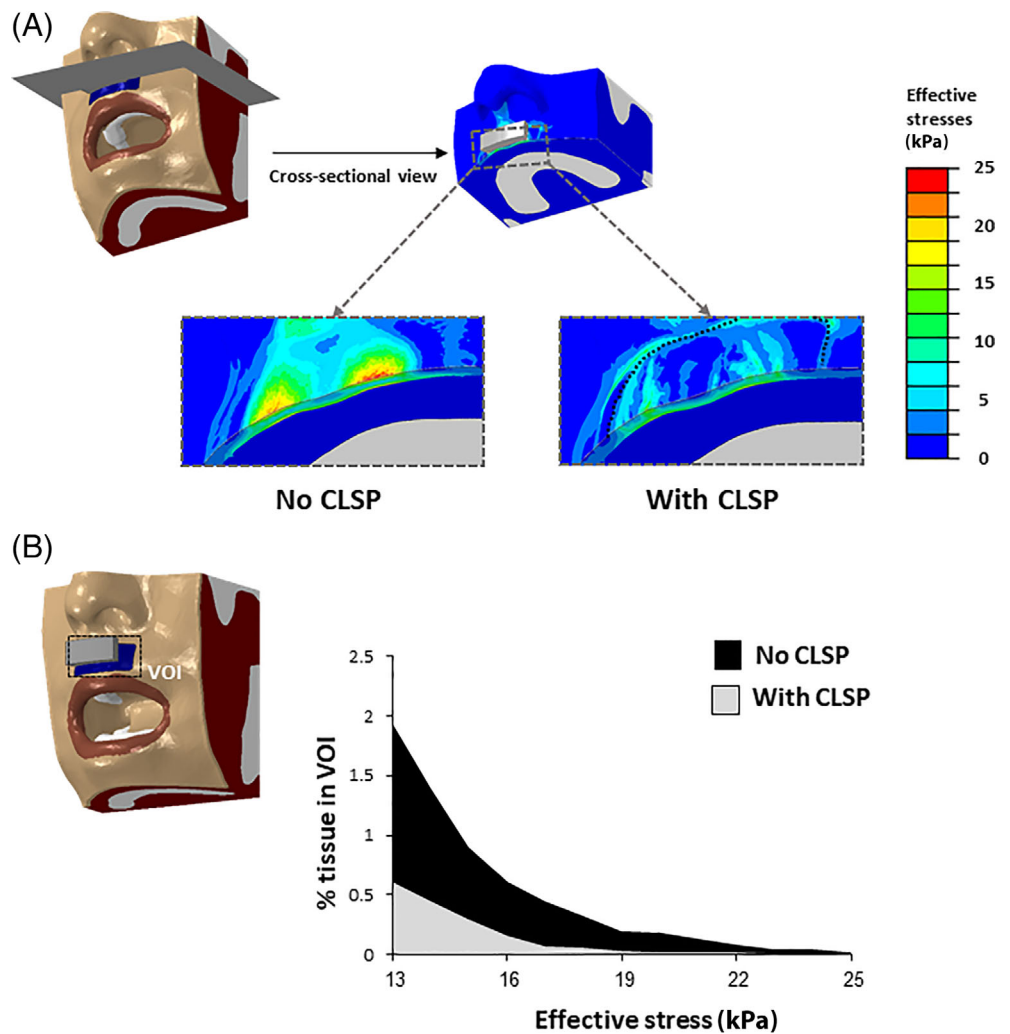


TABLE 2 Cumulative volumetric exposures to effective stresses for skin and cartilage tissues in the ear (in percentage of the total volume of interest), in the model variants without versus with application of cyanoacrylate liquid skin protectant (CLSP)

	Skin		Cartilage	
	Above median	Above the fourth quartile	Above median	Above the fourth quartile
No CLSP (%)	2.52	0.17	6.91	0.44
With CLSP (%)	0.5 (↓ 80%)	0.0053 (↓ 97%)	4.78 (↓ 31%)	0.33 (↓ 25%)

Note: The percentage decrease in tissue stress value as a result of application of the CLSP with respect to the no-CLSP case is provided in brackets.

TABLE 3 Sensitivity analysis of the ear model that included (i) variation of the skin elastic modulus by $\pm 30\%$; (ii) variation of the cyanoacrylate liquid skin protectant (CLSP) elastic modulus by ± 2 SDs around the mean experimental value; and (iii) multiplication of the CLSP thickness by factors of 2 or 3

Model variant	Simulation case description	Percentage tissue volume (skin) where effective stresses exceeded the median stress	Percentage tissue volume (skin) where effective stresses exceeded the fourth-quartile stress	Maximum effective stress value (kPa)	Location of maximum stress
Reference case	No CLSP	2.52	0.17	83.3	UTC
	With CLSP	0.5 (↓ 80%)	0.0053 (↓ 97%)	52.6 (↓ 37%)	BOC
Skin stiffness +30%	No CLSP	2.95	0.33	85.3	UTC
	With CLSP	0.75 (↓ 75%)	0.008 (↓ 97%)	54 (↓ 37%)	BOC
Skin stiffness -30%	No CLSP	1.72	0.083	70.9	UTC
	With CLSP	0.33 (↓ 81%)	0.005 (↓ 94%)	50.1 (↓ 29%)	BOC
CLSP elastic modulus +2 σ	With CLSP	0.45 (↓ 82% ^a)	0.0048 (↓ 97% ^a)	54.4 (↓ 35% ^a)	BOC
CLSP elastic modulus -2 σ	With CLSP	0.54 (↓ 79% ^a)	0.0044 (↓ 97% ^a)	51.2 (↓ 39% ^a)	UTC
CLSP thickness $\times 2$	With CLSP	0.31 (↓ 88% ^a)	0.0048 (↓ 97% ^a)	54 (↓ 35% ^a)	BOC
CLSP thickness $\times 3$	With CLSP	0.27 (↓ 89% ^a)	0.006 (↓ 97% ^a)	57.6 (↓ 31% ^a)	BOC

Note: The percentage decrease in values as a result of application of the CLSP with respect to the corresponding value for the no-CLSP case is provided in brackets.

Abbreviations: BOC, border of CLSP application site; UTC, under the cannula.

^aWith respect to the reference case of no CLSP.

relatively mild reductions in skin stresses with each added CLSP layer, the present results do not appear to support a practice of repetitive applications to build a growing thickness of the CLSP on skin.

3.2 | The mouth region model

The effective stress distributions developed in the tissues of the mouth region model are shown in Figure 9. Again, the stress concentrations that form under the ETAD in the VOIs are evident, but have also been magnified for detail (bottom frames). The highest stresses developed in facial skin of the lateral ridges of the philtrum area, under the borders of the ETAD foam due to its frictional contact with the skin. The model without the CLSP demonstrated considerably greater skin stress levels at the lateral ridges of the philtrum area with respect to the case

TABLE 4 Cumulative volumetric exposures to effective stresses for skin in the upper lip (in percentage of the total volume of interest), in the model variants without versus with application of the cyanoacrylate liquid skin protectant (CLSP)

	Above median	Above the fourth quartile
No CLSP (%)	6.37	1.08
With CLSP (%)	1.75 (↓ 73%)	0.17 (↓ 84%)

Note: The percentage decrease in tissue stress value as a result of application of the CLSP with respect to the no-CLSP case is provided in brackets.

where the CLSP was applied (Figure 9). A view of the stress state in the deeper facial tissues and quantitative analyses of the stress exposures in the VOIs are provided in Figure 10. These data demonstrate that application of the CLSP not only protects the dermis but also project the protective effect subdermally (Figure 10A).

As in the case of the oxygen cannula, here as well, the CLSP reduced the volumetric exposure of skin to stresses across the entire stress domain. The protective effect of the CLSP was substantial for stresses above 13 kPa; skin stress peaks above 23 kPa, which existed for the no-CLSP case were eliminated following application of the CLSP (Figure 10B).

The cumulative volumetric tissue exposures to effective stresses in the VOIs of the mouth region model are specified in Table 4. The CLSP has been shown to reduce skin stresses above the median stress level (13 kPa) and above the fourth-quartile stress value (19 kPa) by $\sim 73\%$ and $\sim 84\%$, respectively. Sensitivity analyses of this mouth region model overall showed trends of effects that were similar to those reported for the ear model earlier.

4 | DISCUSSION

In this work, we investigated the biomechanical protective effect of CLSP against facial MDRPUs using an integrated experimental-computational approach. For the purpose of accurately representing the studied CLSP in our modelling work, we have measured the elastic modulus of the CLSP layer and further tested the COF of this layer (applied on excised animal skin) with medical device materials. We focused on two common sites of facial MDRPUs: the ear and the mouth region. For these facial sites, we have compared tissue stress exposures at each location during contact with a relevant medical device (oxygen cannula for the ear, ETAD for the mouth), between conditions where the CLSP has been applied or where the device was contacting the skin directly, without the shielding of the CLSP. The stress concentration patterns that formed in the skin conformed to the regions of contact with the aforementioned devices and their sites of development were the same sites where MDRPUs associated with oxygen cannulas and usage of ETAD appear in real-world conditions (Figure 3A and Figure 4A, respectively). Accordingly and as expected, tissue stress concentrations associated with the compression and shearing applied by the devices were observed in the modelling under the two device types, with the highest stress values appearing in the superficial skin layers. Notably, the studied CLSP provided highly effective protection from these stress concentrations, by substantially reducing the volumetric soft tissue exposure to stresses under both the oxygen cannula (Figures 5-8) and the ETAD (Figures 9-10). Specifically, for both device/model types, the volumetric skin tissue exposure has been substantially reduced post application of the CLSP, by 73% to 80% for stresses above the median and by 83% to 97% for stresses that make the fourth quartile of the stress range,

which indicates a strong biomechanical efficacy of the studied CLSP in protecting facial skin from MDRPUs.

The above protective effect achieved by the studied CLSP is associated with two primary biomechanical mechanisms that act synergistically²¹: (a) a stress shielding effect where the applied CLSP adds a stiff polymerised layer, which increases the flexural stiffness of skin under external compressive forces; and (b) a COF reduction effect where the smooth polymerised surface of the CLSP reduces the frictional forces between a medical device and the skin under the device. Regarding the first mechanism, the more than 3 orders of magnitude stiffer CLSP layer ($\mu = 59.1$ MPa; Table 1) with respect to the underlying facial skin ($\mu = 50.2$ kPa; Table 1) effectively shielded the skin (despite being only 20 μm thin) to reduce the stress concentrations and volumetric tissue exposure to stresses under the medical devices, as predicted from a theoretical framework that has been previously developed in this regard.²¹ This has also been confirmed in recent work by the Gibson group who used porcine skin specimens and a gel-based skin tissue substitute to test the coating structure and mechanical endurance of the specific CLSP product studied here.^{22,23} With regard to the second mechanism, our present experimental work revealed that application of the CLSP caused a reduction of the COF with medical device materials that is as high as 39% to 58%, which is substantial enough to considerably lower frictional (shear) forces applied by the medical devices to facial skin.^{24,53,55-57} The results of the present work are of high relevance to cases of fragile skin, which is seen in some skin diseases (eg diabetes with ischaemia and neuropathy or epidermolysis bullosa), post-neural-injury skin atrophies or, most frequently, at old age. A fragile skin is particularly thin, weak, and susceptible to abrasion injuries. Application of CLSP on a skin at such condition can compensate for the compromised mechanical strength of skin and also smoothen the wrinkly structure of the elder skin, which mitigates the inherently higher COF of skin associated with the greater surface roughness at old age. Importantly, the above performance characteristics cannot be generalised to any existing or future CLSP technology, as it is specific to the CLSP technology and product that has been studied here. Other products may exhibit different stiffness properties, COF characteristics, or thickness of the polymerised layer on skin; each of these features and their combined effect have a strong influence on the stress state of tissues, as demonstrated throughout this work.

One of the sensitivity analyses conducted here specifically tested the effect of the CLSP thickness on the resulting protective effect (Figure 8). Re-application of CLSP on top of a previously polymerised CLSP layer at short time intervals (ie not for replacing a layer that had

washed-off which, according to the manufacturer, occurs after 3 days) may increase the flexural stiffness of the CLSP coating and thereby shield the skin better. On the other hand, however, such re-application consumes more nursing time, which is a more expensive resource with respect to the cost of the disposable CLSP itself.⁵⁸ This makes the issue of re-application of the CLSP an interesting cost-benefit problem. Our present findings (Figure 8) revealed only mild improvement in the volumetric tissue exposure to stress after reapplying the CLSP for a second or a third time (detailed data were provided in Table 3), yielding that there is no biomechanical justification for a clinical practice of repetitive applications to build a growing thickness of a CLSP coating on the skin.

The important limitations associated with the modelling assumptions and techniques are as follows: (a) the geometries considered for the ear and mouth models represent a specific head and facial anatomy. (b) We did not consider the sublayers of skin or its microtopographical features. (c) We did not directly consider any effects of moisture on the function of the CLSP or the integrity of tissues, or both. All these topics are important and warrant further research to consider anatomical variations in facial contours (which may in turn depend on gender and ethnicity); aging effects on skin wrinkling (possibly using a hierarchical modelling approach); and the influence of moisture exposures on the stiffness and COF properties of the CLSP in interaction with the skin. With that said, the present modelling is the most advanced work to date in MDRPU in silico research and, in particular, is the first ever to test the biomechanical efficacy of CLSP in protecting against PUs and facial MDRPUs in particular.

In conclusion, through combined experimental and computational work, this study demonstrated a strong biomechanical efficacy of the studied CLSP in protecting against facial MDRPUs. The studied CLSP product shields the skin from both compressive and frictional (shearing) contact forces that are associated with skin-contacting medical devices and substantially lowers the stress exposures of skin under (commonly used) devices at the sites of application. The chosen facial anatomical sites studied here, that is, above the ear and between the mouth and nose, are difficult to protect by other means, the first because the region is small and highly curved and the second due to continuous presence of moisture and wetness. Accordingly, the presently studied CLSP provides a unique preventative solution for these problematic facial sites, which is shown here to be highly effective.

ACKNOWLEDGEMENTS

This work was partially supported by an unrestricted educational grant from Medline Industries, Inc. (Northfield IL, USA) and by the Israeli Ministry of Science & Technology

(Medical Devices Program Grant no. 3-17421, awarded to Professor Amit Gefen in 2020).

DATA AVAILABILITY STATEMENT

The data that support the findings of this study are available from the corresponding author upon reasonable request.

ORCID

Amit Gefen  <https://orcid.org/0000-0002-0223-7218>

REFERENCES

- Gefen A, Brienza D, Edsberg L, et al. *Prevention and Treatment of Pressure Ulcers/Injuries: Clinical Practice Guideline*. In: Haesler E. Westford, MA: European Pressure Ulcer Advisory Panel (EPUAP), National Pressure Injury Advisory Panel (NPIAP) and the Pan Pacific Pressure Injury Alliance (PPPIA); 2019. Etiology chapter, pp. 16–27.
- Gefen A, Alves P, Ciprandi G, et al. Device-related pressure ulcers: SECURE prevention. *J Wound Care*. 2020;29(Sup2a):S1-S52. <https://doi.org/10.12968/jowc.2020.29.Sup2a.S1>
- Barakat-Johnson M, Lai M, Wand T, Li M, White K, Coyer F. The incidence and prevalence of medical device-related pressure ulcers in intensive care: a systematic review. *J Wound Care*. 2019;28(8):512-521.
- Jackson D, Sarki AM, Betteridge R, Brooke J. Medical device-related pressure ulcers: a systematic review and meta-analysis. *Int J Nurs Stud*. 2019;92:109-120. <https://doi.org/10.1016/j.ijnurstu.2019.02.006>
- Apold J, Rydrych D. Preventing device-related pressure ulcers. *J Nurs Care Qual*. 2012;27(1):28-34. <https://doi.org/10.1097/NCQ.0b013e31822b1fd9>
- Barakat-Johnson M, Barnett C, Wand T, White K. Medical device-related pressure injuries: an exploratory descriptive study in an acute tertiary hospital in Australia. *J Tissue Viability*. 2017;26(4):246-253. <https://doi.org/10.1016/j.jtv.2017.09.008>
- Turjanica MA, Clark L, Martini C, Miller P, Turner BL, Jones S. Incidence, correlates, and interventions used for pressure ulcers of the ear. *Medsurg Nurs*. 2011;20(5):241-246.
- Black JM, Cuddigan JE, Walko MA, Didier LA, Lander MJ, Kelpel MR. Medical device related pressure ulcers in hospitalized patients. *Int Wound J*. 2010;7(5):358-365. <https://doi.org/10.1111/j.1742-481X.2010.00699.x>
- Hampson J, Green C, Stewart J, et al. Impact of the introduction of an endotracheal tube attachment device on the incidence and severity of oral pressure injuries in the intensive care unit: a retrospective observational study. *BMC Nurs*. 2018;17(1):1-8. <https://doi.org/10.1186/s12912-018-0274-2>
- Landsperger JS, Byram JM, Lloyd BD, Rice TW, Janz DR. The effect of adhesive tape versus endotracheal tube fastener in critically ill adults: the endotracheal tube securement (ETTS) randomized controlled trial. *Crit Care*. 2019;23(1):1-7. <https://doi.org/10.1186/s13054-019-2440-7>
- Kuniavsky M, Vilenchik E, Lubanetz A. Under (less) pressure – facial pressure ulcer development in ventilated ICU patients: a prospective comparative study comparing two types of endotracheal tube fixations. *Intensive Crit Care Nurs*. 2020;58:102804. <https://doi.org/10.1016/j.iccn.2020.102804>

12. Yamashita M, Nishio A, Daizo H, Kishibe M, Shimada K. Intraoperative acquired pressure ulcer on lower lip. *J Craniofac Surg.* 2014;25(1):e3-e4. <https://doi.org/10.1097/SCS.0b013e3182a2ec23>
13. Siotos C, Bonett AM, Hansdorfer MA, Siotou K, Kambeyanda RH, Dorafshar AH. Medical device related pressure ulcer of the lip in a patient with COVID-19: Case report and review of the literature. *J Stomatol Oral Maxillofac Surg.* 2020;8. <https://doi.org/10.1016/j.jormas.2020.09.020>
14. Padula WV, Delarmente BA. The national cost of hospital-acquired pressure injuries in the United States. *Int Wound J.* 2019;16(3):634-640. <https://doi.org/10.1111/iwj.13071>
15. Voss AC, Bender SA, Ferguson ML, Sauer AC, Bennett RG, Hahn PW. Long-term care liability for pressure ulcers. *J Am Geriatr Soc.* 2005;53(9):1587-1592. <https://doi.org/10.1111/j.1532-5415.2005.53462.x>
16. Ayello EA, Capitulo KL, Fife CE, et al. Legal issues in the Care of Pressure Ulcer Patients: key concepts for health care providers: a consensus paper from the international expert wound care advisory panel. *J Palliat Med.* 2009;12(11):995-1008. <https://doi.org/10.1089/jpm.2009.9939>
17. Black J, Cheatle K. Ten top tips: preventing pressure ulcers in the surgical patient - wounds international. *Wounds Int.* 2016;7(3):11-17.
18. Peko Cohen L, Ovadia-Blechman Z, Hoffer O, Gefen A. Dressings cut to shape alleviate facial tissue loads while using an oxygen mask. *Int Wound J.* 2019;16(3):813-826. <https://doi.org/10.1111/iwj.13101>
19. Vlahovic TC, Hinton EA, Chakravarthy D, Fleck CA. A review of cyanoacrylate liquid skin protectant and its efficacy on pedal fissures. *J Am Col Certif Wound Spec.* 2010;2(4):79-85. <https://doi.org/10.1016/j.jcws.2011.02.003>
20. Milne CT, Saucier D, Trevellini C, Smith J. Evaluation of a cyanoacrylate dressing to manage Peristomal skin alterations under Ostomy skin barrier wafers. *J Wound Ostomy Cont Nurs.* 2011;38(6):676-679. <https://doi.org/10.1097/WON.0b013e318234550a>
21. Gefen A. The bioengineering theory of the key modes of action of a cyanoacrylate liquid skin protectant. *Int Wound J.* 2020;17(5):1396-1404. <https://doi.org/10.1111/iwj.13401>
22. Lee J, Gibson DJ. A comparison of the biomechanical protection provided by 2 cyanoacrylate-based skin protectants. *J Wound Ostomy Cont Nurs.* 2020;47(2):118-123. <https://doi.org/10.1097/WON.0000000000000618>
23. Gibson DJ. An ex vivo comparison of 2 cyanoacrylate skin protectants. *J Wound Ostomy Cont Nurs.* 2018;45(1):31-36. <https://doi.org/10.1097/WON.0000000000000391>
24. Schwartz D, Magen YK, Levy A, Gefen A. Effects of humidity on skin friction against medical textiles as related to prevention of pressure injuries. *Int Wound J.* 2018;15(6):866-874. <https://doi.org/10.1111/iwj.12937>
25. Pass DA. Normal anatomy of the avian skin and feathers. *Semin Avian Exot Pet Med.* 1995;4(4):152-160. [https://doi.org/10.1016/S1055-937X\(05\)80013-1](https://doi.org/10.1016/S1055-937X(05)80013-1)
26. Synopsys, Simpleware software solutions - 3D image processing solutions. <https://www.synopsys.com/simpleware.html>. Accessed October 11, 2020
27. Visible Human Project® Gallery. https://www.nlm.nih.gov/research/visible/visible_gallery.html. Accessed October 11, 2020.
28. Fletcher J. Dressings: cutting and application guide. <http://www.worldwidewounds.com/2007/may/Fletcher/Fletcher-Dressings-Cutting-Guide.html>. Accessed June 24, 2021)
29. Thompson PS. Nasal Cannula Assembly. US Patent US7614401B2; 2009.
30. Amrani G, Gefen A. Which endotracheal tube location minimises the device-related pressure ulcer risk: the Centre or a corner of the mouth? *Int Wound J.* 2020;17(2):268-276. <https://doi.org/10.1111/iwj.13267>
31. Katzengold R, Gefen A. What makes a good head positioner for preventing occipital pressure ulcers. *Int Wound J.* 2018;15(2):243-249. <https://doi.org/10.1111/iwj.12857>
32. Friedman R, Haimy A, Gefen A, Epstein Y. Three-dimensional biomimetic head model as a platform for thermal testing of protective goggles for prevention of eye injuries. *Clin Biomech.* 2019;64:35-41. <https://doi.org/10.1016/j.clinbiomech.2018.04.012>
33. Flynn C, Taberner AJ, Nielsen PMF, Fels S. Simulating the three-dimensional deformation of in vivo facial skin. *J Mech Behav Biomed Mater.* 2013;28:484-494. <https://doi.org/10.1016/j.jmbbm.2013.03.004>
34. Sopher R, Nixon J, Gorecki C, Gefen A. Exposure to internal muscle tissue loads under the ischial tuberosities during sitting is elevated at abnormally high or low body mass indices. *J Biomech.* 2010;43(2):280-286. <https://doi.org/10.1016/j.jbiomech.2009.08.021>
35. Bos EJ, Pluemeekers M, Helder M, et al. Structural and mechanical comparison of human ear, alar, and septal cartilage. *Plast Reconstr Surg Glob Open.* 2018;6(1):e1610. <https://doi.org/10.1097/GOX.0000000000001610>
36. Luboz V, Promayon E, Payan Y. Linear elastic properties of the facial soft tissues using an aspiration device: towards patient specific characterization. *Ann Biomed Eng.* 2014;42(11):2369-2378. <https://doi.org/10.1007/s10439-014-1098-1>
37. Gefen A, Haberman E. Viscoelastic properties of ovine adipose tissue covering the gluteus muscles. *J Biomech Eng.* 2007;129(6):924-930. <https://doi.org/10.1115/1.2800830>
38. Ferreira JM, Silva H, Costa JD, Richardson M. Stress analysis of lap joints involving natural fibre reinforced interface layers. *Compos Part B Eng.* 2005;36(1):1-7. <https://doi.org/10.1016/j.compositesb.2004.04.011>
39. Moore DF, Jérusalem A, Nyein M, Noels L, Jaffee MS, Radovitzky RA. Computational biology - modeling of primary blast effects on the central nervous system. *Neuroimage.* 2009;47(Suppl. 2):T10-T20. <https://doi.org/10.1016/j.neuroimage.2009.02.019>
40. Horgan TJ, Gilchrist MD. The creation of three-dimensional finite element models for simulating head impact biomechanics. *Int J Crashworthiness.* 2003;8(4):353-366. <https://doi.org/10.1533/ijcr.2003.0243>
41. Koda S, Yamashita K, Matsumoto K, Nomura H. Characterization of polyvinylchloride by means of sound velocity and longitudinal modulus measurements. *Jpn J Appl Phys.* 1993;32(5S):2234-2237. <https://doi.org/10.1143/JJAP.32.2234>
42. Peko Cohen L, Gefen A. Deep tissue loads in the seated buttocks on an off-loading wheelchair cushion versus air-cell-based and foam cushions: finite element studies. *Int Wound J.* 2017;14(6):1327-1334. <https://doi.org/10.1111/iwj.12807>
43. SIMULIA User Assistance 2020 - Abaqus. https://help.3ds.com/2020/english/DSSIMULIA_Established/SIMULIA_Established_FrontmatterMap/sim-r-DSDocAbaqus.htm?ContextScope=all&id=22f51b12ef9f40eb9a179d827295449d#Pg0. Accessed October 10, 2020.

44. Joodaki H, Panzer MB. Skin mechanical properties and modeling: A review. *Proc Inst Mech Eng Part H: J Eng Med.* 2018;232(4):323-343. <https://doi.org/10.1177/0954411918759801>
45. Zhang M, Mak AFT. In vivo friction properties of human skin. *Prosthet Orthot Int.* 1999;23(2):135-141. <https://doi.org/10.3109/03093649909071625>
46. Ramalho A, Szekeres P, In: *Tribology International.* Vol 63. London, UK: Elsevier Ltd; 2013:29-33. doi:<https://doi.org/10.1016/j.triboint.2012.08.018>
47. Gefen A, Krämer M, Brehm M, Burckardt S. The biomechanical efficacy of a dressing with a soft cellulose fluff core in prophylactic use. *Int Wound J.* 2020;17:1968-1985. <https://doi.org/10.1111/iwj.13489>
48. Levy A, Schwartz D, Gefen A. The contribution of a directional preference of stiffness to the efficacy of prophylactic sacral dressings in protecting healthy and diabetic tissues from pressure injury: computational modelling studies. *Int Wound J.* 2017;14(6):1370-1377. <https://doi.org/10.1111/iwj.12821>
49. Levy A, Gefen A. Computer modeling studies to assess whether a prophylactic dressing reduces the risk for deep tissue injury in the heels of supine patients with diabetes. *Ostomy Wound Manag.* 2016;62(4):42-52.
50. Levy A, Kopplin K, Gefen A. An air-cell-based cushion for pressure ulcer protection remarkably reduces tissue stresses in the seated buttocks with respect to foams: finite element studies. *J Tissue Viability.* 2014;23(1):13-23. <https://doi.org/10.1016/j.jtv.2013.12.005>
51. Katzungold R, Gefen A. Modelling an adult human head on a donut-shaped gel head support for pressure ulcer prevention. *Int Wound J.* 2019;16(6):1398-1407. <https://doi.org/10.1111/iwj.13203>
52. Lustig M, Wiggermann N, Gefen A. How patient migration in bed affects the sacral soft tissue loading and thereby the risk for a hospital-acquired pressure injury. *Int Wound J.* 2020;17(3):631-640. <https://doi.org/10.1111/iwj.13316>
53. Schwartz D, Gefen A. The biomechanical protective effects of a treatment dressing on the soft tissues surrounding a non-offloaded sacral pressure ulcer. *Int Wound J.* 2019;16(3):684-695. <https://doi.org/10.1111/iwj.13082>
54. Schwartz D, Levy A, Gefen A. A computer modeling study to assess the durability of prophylactic dressings subjected to moisture in biomechanical pressure injury prevention. *Ostomy Wound Manag.* 2018;64(7):18-26. <https://doi.org/10.25270/owm.2018.7.1826>
55. Sopher R, Gefen A. Effects of skin wrinkles, age and wetness on mechanical loads in the stratum corneum as related to skin lesions. *Med Biol Eng Comput.* 2011;49(1):97-105. <https://doi.org/10.1007/s11517-010-0673-3>
56. Shaked E, Gefen A. Modeling the effects of moisture-related skin-support friction on the risk for superficial pressure ulcers during patient repositioning in bed. *Front Bioeng Biotechnol.* 2013;1:9. <https://doi.org/10.3389/fbioe.2013.00009>
57. Haesler E. Evidence summary: low friction fabric for preventing pressure injuries. *Wound Pract Res J Aust Wound Manag Assoc.* 2020;28(2):97-98.
58. Gefen A, Kolsi J, King T, Grainger S, Burns M. Modelling the costbenefits arising from technologyaided early detection of pressure ulcers—wounds international. *Wounds Int.* 2020;11(1):22-29.

How to cite this article: Margi R, Gefen A. Evaluation of facial tissue stresses under medical devices post application of a cyanoacrylate liquid skin protectant: An integrated experimental-computational study. *Int Wound J.* 2022;19(3): 615-632. <https://doi.org/10.1111/iwj.13660>